Adaptive quantized target tracking in wireless sensor networks

**Majdi Mansouri · Ouachani Ilham ·
Hichem Snoussi · Cédric Richard**

Abstract This paper addresses target tracking in wireless sensor networks (WSN) where the observed system is assumed to evolve according to a probabilistic state space model. We propose to improve the use of the variational filtering (VF) by optimally quantizing the data collected by the sensors. Recently, VF has been proved to be suitable to the communication constraints of WSN. Its efficiency relies on the fact that the online update of the filtering distribution and its compression are executed simultaneously. However, this problem has been used only for binary sensor networks neglecting the transmission energy consumption in a WSN and the information relevance of sensor measurements. Our proposed method is intended to jointly estimate the target position and optimize the quantization level under fixed and variable transmitting power. At each sampling instant, the adaptive method provides not only the estimate of the target position by using the VF but gives also the optimal number of quantization bits per observation. The adaptive quantization is achieved by minimizing the predicted Cramér–Rao bound if the transmitting power is constant for all sensors, and optimizing the power scheduling under distortion constraint if this power is variable. The computation of the predicted Cramér–Rao bound is based on the target position

predictive distribution provided by the VF algorithm. The proposed adaptive quantization scheme suggests that the sensors with bad channels or poor observation qualities should decrease their quantization resolutions or simply become inactive in order to save energy.

1 Introduction

Wireless Sensor Networks [1] nodes are powered by small batteries, which are in practical situations non rechargeable, either due to cost limitations or because they are deployed in hostile environments with high temperature, high pollution levels, or high nuclear radiation levels. These considerations enhance energy-saving and energy-efficient WSN designs. One technique to prolong battery lifetime consists of optimizing quantization of measurements collected by sensors. The problem of quantizing observations to estimate a parameter, either the target position or any other physical field (temperature, humidity, . . .), is different from the problem of quantizing a signal for later reconstruction [2]. Instead of reconstructing a signal, our objective is rather estimating the target trajectory using quantized observations.

There has already been a certain amount of research in the area of quantization for target tracking in wireless sensor networks. In [3], authors have derived the optimal number of quantization levels as well as the optimal energy allocation across bits, but they have neglected the information content relevance of measured data. On the other hand, the work in [4] used a VF algorithm to estimate the target position but it assumed that the transmitting power is

M. Mansouri (✉) · H. Snoussi
ICD/LM2S, University of Technology of Troyes, Troyes, France
e-mail: majdi.mansouri@utt.fr

O. Ilham
Insitut Supérieur d'Informatique et des Technologies de Communication Hammam Sousse, Hammam Sousse, Tunisia

C. Richard
Laboratoire FIZEAU UMR CNRS 6525, Université de Nice Sophia–Antipolis, Valbonne, France

the same for all sensors. The approaches proposed in [5, 6] are limited to a particular 1-bit per quantized observation. The work in [7] has considered an increasingly complex activation schemes in an attempt to reduce the consumed energy and the error estimation. In [8], the authors have proposed a "location-centric" method by dynamically dividing the sensor set into geographic groups run by a the cluster head. In the case of multiple observations, they compare the data fusion versus the decision fusion methods. A distributed protocol for the tracking in sensor networks was developed in [9]. This technique organizes sensors in clusters and uses three sensors to participate in data collection to perform the target tracking process.

Target tracking using quantized observations is a nonlinear estimation problem that can be solved using unscented Kalman filter (KF) [10], particle filters (PF) [11] or variational filtering (VF) [12]. Recently, a variational filtering has been proposed for solving the target tracking problem since: (1) it respects the communication constraints of sensor, (2) the online update of the filtering distribution and its compression are simultaneously performed, and (3) it has the nice property to be model-free, ensuring the robustness of data processing.

Concerning the particle filtering (PF) algorithm, the enormous amount of particles has hampered its implementation in wireless sensor networks. In the literature, different methods to approximate the particles distribution were proposed in order to apply the PF in WSN [13–15]. The work in [15] has proposed a message approximating scheme based on the greedy KD-tree approximation. The proposed Gaussian Particle Filtering (GPF) algorithm [13] and the Gaussian Sum Particle Filtering (GSPF) algorithm [14] consist in approximating the posterior distribution by a single Gaussian distribution and a weighted sum of Gaussian distributions respectively. The principal defect of these algorithms is the error propagation through the sensor network, when approximating the particle representation by a few number of Gaussian statistics.

The VF approach was only extended to Binary Sensor Network (BSN) considering a cluster-based scheme [16]. The BSN is based on the binary proximity observation model; it consists of making a binary decision according to the strength of the perceived signal. Hence, only one bit is transmitted for further processing if a target is detected. This work has also been done considering a cluster-based scheme, where sensors are partitioned into clusters [16]. At each sampling instant, only one cluster of sensors is activated according to the prediction made by the VF algorithm. Resource consumption is thus restricted to the activated cluster, where intra-cluster communications are dramatically reduced. Thanks to its power efficiency, the cluster-based scheme is also considered in this paper. As only a part of information is exploited (hard binary

decision), tracking in binary sensor networks suffers from poor estimation performances. Our contribution is twofold: (1) we investigate the impact of the choice of a fixed (in time) quantization level and uniform power on the VF algorithm performances and propose an adaptive quantization scheme; (2) we jointly optimize the power scheduling to minimize the transmission energy consumption in WSNs.

The proposed method provides not only the Bayesian filtering distribution of the target position but also optimizes the quantization level under constant and variable transmitting power. The optimal quantization level is computed by minimizing the predicted Cramér–Rao bound under constant transmitting power, and by optimizing the power scheduling under variable power transmitting.

As the target position is unknown, the Cramér–Rao bound is averaged according to the target position predictive distribution provided online by the VF algorithm. Similarly, the power scheduling is approximated using this predicted information.

The rest of the paper is organized as follows. Section 2 presents the problem statement. The overview of the VF algorithm and the prediction-based cluster activation are described in Sect. 3. Then, the main contribution of this paper which is the adaptive quantization under fixed and variable transmitting power is presented in Sect. 4 Numerical simulations are shown in Sect. 5, and finally concluding remarks are given in Sect. 6.

2 Modeling and problem statement

2.1 Quantized observation model

We assume that WSN is composed of randomly deployed sensor, whose locations $s^i = (s_1^i, s_2^i)$, $i = 1, 2, \ldots, N_s$ are known, N_s is the total number of sensors. Sensor nodes work collaboratively for mobile target tracking , while the sink node gathers the information sensed by the sensor nodes [9, 10, 11]. We are interested in tracking a target position $xb_t = (x_{1,t}, x_{2,t})^T$ at each instant $t (t = 1, \ldots, N$, where N denotes the number of observations). Consider the activated sensor i, its observation γ_t^i is modeled by:

$$\gamma_t^i = K\|\boldsymbol{x}_t - \boldsymbol{s}_t^i\|^\eta + \epsilon_t \tag{1}$$

where ϵ_t is a Gaussian noise with zero mean and a variance σ_ϵ^2, η and K are known constants. The sensor transmits its observation if and only if $R_{min} \le \|\boldsymbol{x}_t - \boldsymbol{s}_t^i\| \le R_{max}$ where R_{max} denotes the maximum distance at which the sensor can detect the target, and R_{min} is the minimum distance from which the sensor can detect the target. Before being transmitted the observation is quantized by partitioning the observation space

into w_t^i intervals $\mathcal{R}_j = [\tau_j(t), \tau_{j+1}(t)]$, where $j \in \{1, \ldots, w_t^i\}$. w_t^i presents the quantization level to be determined. The quantization level w_t^i is sub-indexed by the sampling instant t since it will be optimized online jointly with the target position online estimation. The quantizer, assumed uniform, is specified through: (1) the thresholds $\{\tau_j(t)\}_{j=1}^{j=w_t^i+1}$, where (if $\eta \geq 0$): $\tau_1(t) = KR_{min}^{\eta}$, $\tau_j(t) \leq \tau_{j+1}(t)$ and $\tau_{w_t^i+1}(t) = KR_{max}^{\eta}$; and (2) the quantization rule:

$$y_t^i = d_j \quad \text{if } \gamma_t^i \in [\tau_j(t), \tau_{j+1}(t)] \tag{2}$$

where, the normalized d_j is given by $d_j = \frac{\tau_j(t) + \frac{\Delta}{2}}{\tau_{w_t^i}(t) - \tau_1(t)}$, and $Q()$ is the quantization function. Figure 1 depicts a simple example for the quantized observation model.

Then, the signal received by the CH from the sensor i at the sampling instant t is written as,

$$z_t^i = \beta_t^i . y_t^i + n_t \tag{3}$$

where $\beta_t^i = r_i^{\lambda}$ is the ith sensor channel attenuation coefficient at the sampling instant t, r_i is the transmission distance between the ith sensor and the CH, λ is the path-loss exponent and n_t is a random Gaussian noise with a zero mean and a known variance σ_n^2. Figure 2 summarizes the transmission scheme occurring during the data processing.

2.2 General state evolution model (GSEM)

Instead of the kinematic parametric model [17–19] which is usually used in tracking problems, we employ a General State Evolution Model (GSEM) [12, 20]. This model is more appropriate to practical non-linear and non-gaussian situations where no a priori information on the target velocity or its acceleration is available. The target position $x_t \in \mathbb{R}^{n_x}$ at instant t is assumed to follow a Gaussian model, where the expectation μ_t and the precision matrix λ_t are both random. The randomness of the expectation and the

precision of the target position is used here to further capture the uncertainty of the state distribution. A practical choice of these distributions is a Gaussian distribution for the expectation and a n_x-dimensional Wishart distribution for the precision matrix. In other words, the hidden state x_t is extended to an augmented state $\alpha_t = (x_t, \mu_t, \lambda_t)$, yielding this hierarchical model,

$$\begin{cases} x_t \sim \mathcal{N}(\mu_t, \lambda_t) \\ \mu_t \sim \mathcal{N}(\mu_{t-1}, \bar{\lambda}) \\ \lambda_t \sim \mathcal{W}_{n_x}(\bar{V}, \bar{n}) \end{cases} \tag{4}$$

where the fixed hyper-parameters $\bar{\lambda}$, $\bar{n}$ and $\bar{V}$ are respectively the random walk precision matrix, the degrees of freedom and the precision of the Wishart distribution. Assuming a random mean and a random covariance for the state x_t leads to a probability distribution covering a wide range of tail behaviors, which allows discrete jumps in the target trajectory. The GSEM is depicted in Fig. 3.

The next section describes the Bayesian tracking solution based on a Quantized Variational Filtering (QVF) algorithm.

3 Bayesian estimation approach via a QVF

3.1 Overview of the VF algorithm

In this section, we assume that the quantization level is already optimized (see next Sect. 4). Hence, the observation model is completely defined. The aim of this section is to describe the target position estimation procedure.

According to the model (4), the augmented hidden state is now $\alpha_t = (x_t, \mu_t, \lambda_t)$. We consider the posterior distribution $p(\alpha_t|z_{1:t})$, where $z_{1:t} = \{z_1, z_2, \ldots, z_t\}$ denotes the collection of observations gathered until time

Fig. 1 The quantized observation model is described by a simple example. With respect to the first sensor, the target is within its sensing range at instant t. Observation y_t^1 is thus transmitted to the CH. However the second sensor keeps silent. The situation at instant $t + 1$ can be similarly deduced
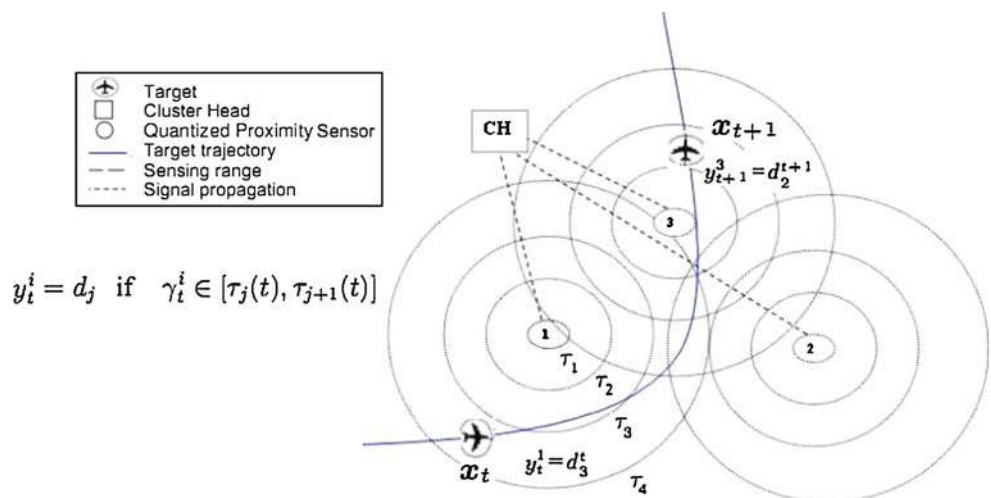

$$y_t^i = d_j \quad \text{if} \quad \gamma_t^i \in [\tau_j(t), \tau_{j+1}(t)]$$

Fig. 2 Illustration of the communications path-ways in a WSN: The 1st sensor makes a noisy reading γ_t^1. The quantized measurement $y_t^1 = Q(\gamma_t^1)$ with L_t^1 bits of precision is sent to the *CH*. The measurement z_t^1 is received by the *CH*, it is corrupted by an additive white Gaussian noise n_t
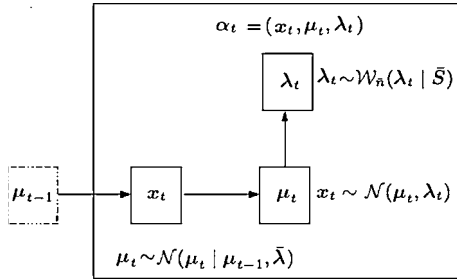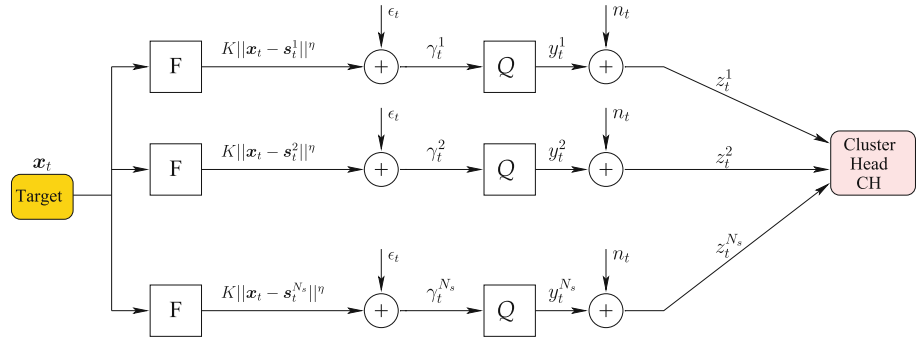

Fig. 3 General state evolution model GSEM

t. The variational approach consists in approximating $p(\boldsymbol{\alpha}_t|z_{1:t})$ by a separable distribution $q(\boldsymbol{\alpha}_t) = \Pi_i q(\boldsymbol{\alpha}_t^i) = q(\boldsymbol{x}_t)q(\boldsymbol{\mu}_t)q(\boldsymbol{\lambda}_t)$ that minimizes the Kullback–Leibler (KL) divergence between the true filtering distribution and the approximate distribution,

$$D_{\mathrm{KL}}(q||p) = \int q(\boldsymbol{\alpha}_t) \log \frac{q(\boldsymbol{\alpha}_t)}{p(\boldsymbol{\alpha}_t|z_{1:t})} d\boldsymbol{\alpha}_t \tag{5}$$

To minimize the KL divergence subject to constraint $\int q(\boldsymbol{\alpha}_t)d\boldsymbol{\alpha}_t = \Pi_i \int q(\boldsymbol{\alpha}_t^i)d\boldsymbol{\alpha}_t^i = 1$, the Lagrange multiplier method is used, yielding the following approximate distribution [12]

$$q(\boldsymbol{\alpha}_t^i) \propto \exp \langle \log p(z_t, \boldsymbol{\alpha}_t) \rangle_{\Pi_{j \neq i} q(\boldsymbol{\alpha}_t^i)} \tag{6}$$

where $\langle . \rangle_{q(\boldsymbol{\alpha}_t^i)}$ denotes the expectation operator relative to the distribution $q(\boldsymbol{\alpha}_t^i)$.

Taking into account the separable approximate distribution $q(\boldsymbol{\alpha}_{t-1})$ at time $t-1$, the filtering distribution $p(\boldsymbol{\alpha}_t|z_{1:t})$ is sequentially approximated according to the (7) (see Appendix for details):

$$\hat{p}(\boldsymbol{\alpha}_t|z_{1:t}) = \frac{p(z_t|\boldsymbol{\alpha}_t) \int p(\boldsymbol{\alpha}_t|\boldsymbol{\alpha}_{t-1})q(\boldsymbol{\alpha}_{t-1})d\boldsymbol{\alpha}_{t-1}}{p(z_t|z_{1:t-1})}$$

$$\propto p(z_t|\boldsymbol{x}_t)p(\boldsymbol{x}_t|\boldsymbol{\mu}_t, \boldsymbol{\lambda}_t)p(\boldsymbol{\lambda}_t)q_p(\boldsymbol{\mu}_t), \tag{7}$$

with $q_p(\boldsymbol{\mu}_t) = \int p(\boldsymbol{\mu}_t|\boldsymbol{\mu}_{t-1})q(\boldsymbol{\mu}_{t-1})d\boldsymbol{\mu}_{t-1}$.

Therefore, through a simple integral with respect to μ_{t-1}, the filtering distribution $p(\boldsymbol{\alpha}_t|z_{1:t})$ can be sequentially updated. Considering the GSEM proposed in above, the

evolution of $q(\mu_{t-1})$ is Gaussian, namely $p(\mu_t|\mu_{t-1}) \sim \mathcal{N}(\boldsymbol{\mu}_{t-1}, \overline{\boldsymbol{\lambda}})$. Defining $q(\mu_{t-1}) \sim \mathcal{N}(\boldsymbol{\mu}_{t-1}^*, \boldsymbol{\lambda}_{t-1}^*)$, $q_p(\mu_t)$ is also Gaussian (see Appendix for details), with the parameters,

$$q_p(\boldsymbol{\mu}_t) \sim \mathcal{N}(\boldsymbol{\mu}_t^p, \boldsymbol{\lambda}_t^p)$$

where $\boldsymbol{\mu}_t^p = \boldsymbol{\mu}_{t-1}^*$ and $\boldsymbol{\lambda}_t^p = (\boldsymbol{\lambda}_{t-1}^{*-1} + \overline{\boldsymbol{\lambda}}^{-1})^{-1}$ \tag{8}

The temporal dependence is hence reduced to the incorporation of only one Gaussian component approximation $q_p(\mu_{t-1})$. The update and the approximation of the filtering distribution $p(\boldsymbol{\alpha}_t|z_{1:t})$ are jointly performed, yielding a natural and adaptive compression [21]. According to the (6), variational calculus leads to this iterative solution (see Appendix):

$$q(\boldsymbol{x}_t) \propto p(z_t|\boldsymbol{x}_t)\mathcal{N}(\boldsymbol{x}_t|\langle \boldsymbol{\mu}_t \rangle, \langle \boldsymbol{\lambda}_t \rangle)$$
$$q(\boldsymbol{\mu}_t) \propto \mathcal{N}(\boldsymbol{\mu}_t|\boldsymbol{\mu}_t^*, \boldsymbol{\lambda}_t^*)$$
$$q(\boldsymbol{\lambda}_t) \propto \mathcal{W}_{n^*}(\boldsymbol{\lambda}_t|\boldsymbol{S}_t^*)$$
$$q(\boldsymbol{\mu}_t|\boldsymbol{\mu}_{t-1}) \propto \mathcal{N}(\boldsymbol{\mu}_t^p, \boldsymbol{\lambda}_t^p)$$

where the parameters are iteratively updated according to the following scheme:

$$\boldsymbol{\mu}_t^* = \boldsymbol{\lambda}_t^{*-1}(\langle \boldsymbol{\lambda}_t \rangle \langle \boldsymbol{x}_t \rangle + \boldsymbol{\lambda}_t^p \boldsymbol{\mu}_t^p)$$
$$\boldsymbol{\lambda}_t^* = \langle \boldsymbol{\lambda}_t \rangle + \boldsymbol{\lambda}_t^p$$
$$n^* = \bar{n} + 1$$
$$\boldsymbol{S}_t^* = (\langle \boldsymbol{x}_t \boldsymbol{x}_t^T \rangle - \langle \boldsymbol{x}_t \rangle \langle \boldsymbol{\mu}_t \rangle^T - \langle \boldsymbol{\mu}_t \rangle \langle \boldsymbol{x}_t \rangle^T + \langle \boldsymbol{\mu}_t \boldsymbol{\mu}_t^T \rangle + \bar{\boldsymbol{S}}^{-1})^{-1}$$
$$\boldsymbol{\mu}_t^p = \boldsymbol{\mu}_{t-1}^*$$
$$\boldsymbol{\lambda}_t^p = (\boldsymbol{\lambda}_{t-1}^{*-1} + \overline{\boldsymbol{\lambda}}^{-1})^{-1}$$

3.2 Prediction-based cluster activation using the VF algorithm

The main advantage of the variational approach is the compression of the statistics required for the update of the filtering distribution between two successive instants. This implicit compression makes the variational algorithm adapted to be distributively implemented through the network. In other words, it can be executed on a cluster-base which is considered in this paper. The cluster head is here

determined based on the predicted target position given by the VF algorithm. Indeed,after updating the VF distribution, the role of the cluster head CH_t (at the sampling instant t) is to calculate the predictive distribution. The predictive distribution can be efficiently updated by the VF approach. In fact, taking into account the separable approximate distribution at time $t - 1$, the predictive distribution is written,

$$p(\boldsymbol{\alpha}_t|z_{1:t-1}) \propto p(\boldsymbol{x}_t, \lambda_t|\boldsymbol{\mu}_t) \int p(\boldsymbol{\mu}_t|\boldsymbol{\mu}_{t-1}) q(\boldsymbol{\mu}_{t-1}) d\boldsymbol{\mu}_{t-1} \quad (9)$$

The exponential form solution, which minimizes the Kullback–Leiblerdivergence between the predictive distribution $p(\boldsymbol{\alpha}_t|z_{1:t-1})$ and the separable approximate distribution $q_{t|t-1}(\boldsymbol{\alpha}_t)$, yields Gaussian distributions for the state and its mean and Wishart distribution for the precision matrix:

$$q_{t|t-1}(\boldsymbol{x}_t) \propto \mathcal{N}(\boldsymbol{x}_t|\langle\boldsymbol{\mu}_t\rangle, \langle\lambda_t\rangle)$$
$$q_{t|t-1}(\boldsymbol{\mu}_t) \propto \mathcal{N}(\boldsymbol{\mu}_t|\boldsymbol{\mu}_t^*, \lambda_t^*) \quad (10)$$
$$q_{t|t-1}(\lambda_t) \propto \mathcal{W}_{n^*}(\lambda_t|S_t^*)$$

where the parameters are updated according to the same iterative scheme as in (9) and the expectations are exactly computed as,

$$\langle\boldsymbol{x}_t\rangle_{q_{t|t-1}} = \langle\boldsymbol{\mu}_t\rangle_{q_{t|t-1}},$$
$$\langle\boldsymbol{x}_t\boldsymbol{x}_t^T\rangle_{q_{t|t-1}} = \langle\boldsymbol{\mu}_t\rangle_{q_{t|t-1}} + \langle\boldsymbol{\mu}_t\rangle_{q_{t|t-1}} \langle\boldsymbol{\mu}_t\rangle_{q_{t|t-1}}^T. \quad (11)$$

Hence, the QVF provides at the sampling instant t, the predicted target position $\boldsymbol{x}_{t/t-1} = \langle\boldsymbol{x}_t\rangle_{q_{t|t-1}}$. As shown in Fig. 4, based on the predicted target position $\langle\boldsymbol{x}_t\rangle_{q_{t|t-1}}$, the cluster head CH_{t-1} at sampling instant $t - 1$, selects the next cluster head CH_t. If the predicted target position $\langle\boldsymbol{x}_t\rangle_{q_{t|t-1}}$ remains in the vicinity of CH_{t-1}, which means that at least four of its salve sensors can detect the target [22], then $CH_t = CH_{t-1}$. Otherwise, if $\l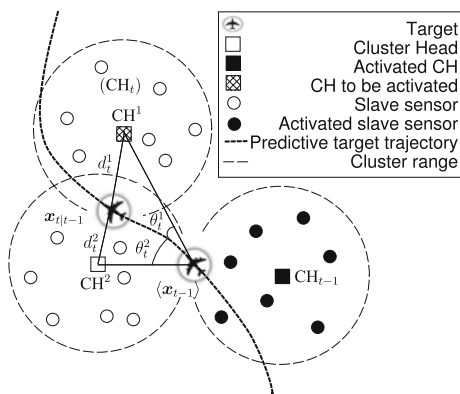angle\boldsymbol{x}_t\rangle_{q_{t|t-1}}$ is going beyond the sensing range of the current cluster, then a new CH_t is activated, based on the target position prediction $\langle\boldsymbol{x}_t\rangle_{q_{t|t-1}}$ and its future tendency.

$$CH_t = \underset{k=1,\dots,K}{\operatorname{argmax}} \left\{ \frac{\cos\theta_t^k}{d_t^k} \right\}$$
where $d_t^k = \|\langle\boldsymbol{x}_t\rangle_{q_{t|t-1}} - L_{CH_t^k}\|$ \quad (12)
and $\theta_t^k = angle(\overrightarrow{\langle\boldsymbol{x}_{t-1}\rangle\langle\boldsymbol{x}_t\rangle_{q_{t|t-1}}}, \overrightarrow{\langle\boldsymbol{x}_{t-1}\rangle L_{CH_t^k}})$

where K is the number of CHs in the neighborhood of CH_{t-1} and L_{CH^k} is the location of the kth neighboring CH_t. The next section is devoted to the developed method aimed at adaptively (and jointly) optimizing the number of quantization bits per observation.

4 Adaptive quantization for target tracking

The key idea behind the optimization of the quantization is that under constant or variable transmitting power, a higher quantization level could affect the estimation performances. In fact, a quantizer is identified with quantization level N_t^i, the decision boundaries τ_j and the corresponding representation values d_j. If the quantization level increases, the quantized values d_j are very close and the distance between the symbols decreases. Hence, a small noise could affect the decision rule, thus the estimation error increases (see Fig. 5).

At sampling time $t - 1$, the selected cluster head CH_{t-1} executes the VF algorithm and provides the Gaussian predictive distribution $\mathcal{N}(\boldsymbol{x}_{t/t-1}, \lambda_{t/t-1})$. The predicted position allows the selection of the cluster to be activated

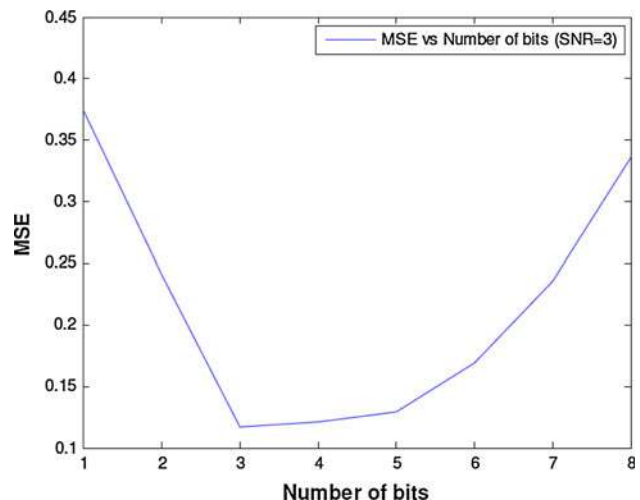**Fig. 4** Prediction-based CH_t activation

Fig. 5 MSE versus the number of quantization bits (fixed in time) varying in $\{1, 2, \dots, 8\}$ for SNR = 3

as described in Sect. 3.2. Furthermore, this target position is used by the CH_{t-1} to give the optimal quantization level $\widehat{w}_t^i$ minimizing the predicted Cramér–Rao bound where the transmission power is constant. When this transmitting power is variable, the optimal of quantization level is computed by optimizing the power scheduling. This optimal quantization level is then transmitted to the CH_t before being broadcasted to the activated sensors so that they use it to quantize their observations. These quantized observations are then used by the CH_t to execute the VF algorithm at the sampling instant t. In the following, we describe the two techniques in details.

4.1 Optimizing the quantization for constant transmitting powers

Where the transmitting power between sensors is fixed, the optimal quantization level could be obtained by minimizing the Cramér–Rao bound (CRB). This bound is often used to evaluate the efficiency of a given estimator. Inits simplest form, the bound states that the covariance of any estimator is at least higher as the inverse of the Fisher Information (FI) matrix. The FI matrix is a quantity measuring the amount of information that the observable variable z_t^i carries about the unknown parameter x_t. The FI matrix elements at the sampling instant t are given by:

$$\left[\mathrm{FI}\left(x_t, s^i, w_t^i\right) \right]_{l,k} = \left\langle \frac{\partial \log(p(z_t^i|x_t))}{\partial x_{(l,t)}} \frac{\partial \log(p(z_t^i|x_t))}{\partial x_{(k,t)}} \right\rangle_{z_t^i|x_t}$$
$$(l,k) \in \{1,2\} \times \{1,2\} \qquad (13)$$

where z_t^i denotes the observation of the i-th sensor at the sampling instant t, $x_t = [x_1, x_2]^T$ is the unknown 2×1 vector to be estimated, and

$$p\left(z_t^i|x_t\right) = \sum_{j=0}^{w_t^i-1} p\left(\tau_j(t) < \gamma_t^i < \tau_{j+1}(t)\right) \mathcal{N}\left(\beta d_j, \sigma_\epsilon^2\right) \qquad (14)$$

where

$$p\left(\tau_j(t) < \gamma_t^i < \tau_{j+1}(t)\right) = \int_{\tau_j(t)}^{\tau_{j+1}(t)} \mathcal{N}\left(\rho_{\gamma_t^i}(x_t), \sigma_n^2\right) d\gamma_t^i \qquad (15)$$

is computed according to the quantization rule defined in (2), in which

$$\rho_{\gamma_t^i}(x_t) = K \|x_t - s_t^i\|^\eta, \qquad (16)$$

Then, the derivative of the log-likelihood function can be expressed as,

$$\frac{\partial \log(p(z_t^i|x_t))}{\partial x_{l,t}} = \frac{\eta K}{\sqrt{2\sigma_n^2}} (x_{l,t} - s_{l,i}) \|x_{l,t} - s_{l,i}\|^{\eta-2}$$
$$\times \sum_{k=1}^{w_t^i} \left[\exp\left(-\frac{1}{2} \frac{(\tau_k - \rho_{\gamma_t^i}(x_t))^2}{\sigma_n^2} \right) \right.$$
$$\left. - \exp\left(-\frac{1}{2} \frac{(\tau_{k+1} - \rho_{\gamma_t^i}(x_t))^2}{\sigma_n^2} \right) \right]$$
$$\times \exp\left(-\frac{1}{2} \frac{(z_t(k) - d_k)^2}{\sigma_\epsilon^2} \right) \Big/$$
$$\sum_{k=1}^{w_t^i} \left[\mathrm{erfc}\left(\frac{\tau_k - \rho_{\gamma_t^i}(x_t)}{\sqrt{2\sigma_n^2}} \right) \right.$$
$$\left. - \mathrm{erfc}\left(\frac{\tau_{k+1} - \rho_{\gamma_t^i}(x_t)}{\sqrt{2\sigma_n^2}} \right) \right]$$
$$\times \exp\left(-\frac{1}{2} \frac{(z_t(k) - d_k)^2}{\sigma_\epsilon^2} \right) \qquad (17)$$

Substituting expression (17) in (13), the FI matrix is easily computed by integrating over the likelihood function $p\left(z_t^i|x_t\right)$ at the sampling instant t.

It is worth noting that the expression of the FI given in (17) depends on the target position x_t at the sampling instant t and on the quantization level w_t. However, as the target position is unknown, the FI is replaced by its expectation according to the predictive distribution $p\left(x_t|z_{1:t-1}^i\right)$ of the target position:

$$\left\langle \mathrm{FI}\left(x_t, s^i, w_t^i\right) \right\rangle = \left\langle \mathrm{FI}\left(x_t, w_t^i\right) \right\rangle_{p(x_t|z_t^i)} \qquad (18)$$

Computing the above expectation is analytically untractable. However, as the VF algorithm yields a Gaussian predictive distribution $\mathcal{N}(x_t; x_{t/t-1}, \lambda_{t/t-1})$, expectation (18) can be efficiency approximated by a Monte Carlo scheme:

$$\left\langle \mathrm{FI}(x_t, s^i, w_t^i) \right\rangle \simeq \frac{1}{J} \sum_{j=1}^{J} \mathrm{FI}(\tilde{x}_t^j, s^i, w_t^i),$$
$$\tilde{x}_t^j \sim \mathcal{N}(x_p(t); x_{t/t-1}, \lambda_{t/t-1}) \qquad (19)$$

where $\tilde{x}_t^j$ is the jth drawn sample at instant t, and J is the total number of drawn vectors $\tilde{x}_t$.

Then, the CH can compute at the sampling instant t the optimal quantization level used by ith sensor by maximizing the FI matrix:

$$\widehat{w}_t^i = \arg \max(\left\langle \mathrm{FI}(x_t, s^i, w_t^i) \right\rangle). \qquad (20)$$

4.2 Optimizing the quantization for variable transmitting power

Contrary to the previous subsection, we assume here that the transmitting power could be controlled by the sensors.

The objective is then the optimization of the transmitting power while ensuring a good tracking performance. The total amount of the required transmission power used by the ith sensor within a cluster [23] is proportional to:

$$P^i(t) \propto r_i^\lambda \left(w_t^i - 1 \right). \tag{21}$$

The optimal resource allocation problem is expressed as an optimization of the quantization level w_t^i over the field $\mathbf{Z}_+$ subject to an average estimation error constraint M_0,

$$\min_{w_t^i \in \mathbf{Z}_+} \sum_{i=1,\dots,N_a} P^i(t)^2 \tag{22}$$
$$\text{s.t } CRB\left(\mathbf{x}_t, w_t^i\right) < M_0$$

where N_a is the number of activated sensors at instant t.

The Lagrangian formulation of this constrained optimization is expressed as,

$$L = \sum_i r_i^{2\lambda} \left(w_t^i - 1 \right)^2 + \left(\mu CRB\left(\mathbf{x}_t, w_t^i\right) - M_0 \right) \tag{23}$$

where μ is the Lagrange multiplier constant.

Then, the optimal value of $\widehat{w}_t^i$ is a solution of the following equation:

$$f\left(\widehat{w}_t^i\right) = \frac{\partial L}{\partial \widehat{w}_t^i} = \left(\widehat{w}_t^i - 1 \right) - g\left(\widehat{w}_t^i\right) = 0 \tag{24}$$

where $g\left(\widehat{w}_t^i\right)$ denotes $-\frac{\mu}{2r_i^{2\lambda}} \frac{\partial CRB\left(\mathbf{x}_t, \widehat{w}_t^i\right)}{\partial \widehat{w}_t^i}$.

Applying the Newton–Raphson procedure yields the following sequence converging to the solution of (24):

$$\widehat{w}_t^i(n+1) = \widehat{w}_t^i(n) - \frac{f\left(\widehat{w}_t^i(n)\right)}{f'\left(\widehat{w}_t^i(n)\right)}$$
$$= \widehat{w}_t^i(n) - \frac{\left(\widehat{w}_t^i(n) - 1\right) - g\left(\widehat{w}_t^i(n)\right)}{1 - g'\left(\widehat{w}_t^i(n)\right)} \tag{25}$$

The overall proposed method is summarized in Algorithm 1 and its diagram is shown in Fig. 6.

5 Simulation results analysis

The performance of the tracking algorithm can be essentially assessed by the tracking accuracy (detailed in Sect. 5.1), by the Root Mean Square Error (RMSE) (detailed in Sect. 5.2), and by computing the energy expenditure during the whole tracking process (detailed in Sect. 5.3).

In the following, we compare the tracking accuracy of the proposed adaptive quantized variational filter (AQVF) method, with the quantized variational filter processing under an uniform transmitting power (QVF-U), the binary variational filtering (BVF) [24], the centralized quantized gaussian particle filter (QGPF) and the centralized quantized particle filter (QPF). All the simulations shown in this paper are implemented with Matlab version 7.1, using an Intel Pentium CPU 3.4 GHz, 1.0 G of RAM PC.

The system parameters considered in the following simulations are: $\eta = 2$ for free space environment, the constant characterizing the sensor range is fixed for simplicity to $K = 1$, the cluster head noise power is $\sigma_n^2 = 0.05$, the total number of sensors is $N_s = 100$, the total sampling instants is $N = 100$, the sensor noise power is $\sigma_\epsilon^2 = 0.01$, the maximum sensing range R_{max} (resp. the minimum sensing range R_{min}) is fixed to 10 m (resp. 0 m) and 100 particles were used in AQVF, QVF-U, BVF, QGPF and QPF methods.

To investigate the impact of the choice of a fixed (in time) quantization level on the VF algorithm performance, we run the VF algorithm for different fixed quantization levels used per observation and compute the average estimation error over the target trajectory (MSE). Figure 5 plots the MSE versus the number of bits per observation varying in $\{1, 2, \dots, 8\}$. We note that the MSE is minimum for a quantization bit number $\widehat{L} = 3$.

**Algorithm 1** Pseudo-code of the proposed algorithm

— Initialization:

   1) Select sensors

   2) Quantize using an uniform power

   3) Execute the VF algorithm

— Iterations:

   1) Select sensors according to Sub. III-B.

   2) Compute the Cramér–Rao bound based on the predicted target position.

      a) Compute the optimal level quantization by minimizing the CRB, if the transmitting power is constant for all sensors using the equation (25).

      b) Compute the optimal level quantization by optimizing the power scheduling, if the transmitting power is variable using the equation (21).

   3) Quantize using the optimal level quantization.

   4) Execute the VF algorithm.

Fig. 6 A global overview of the proposed method
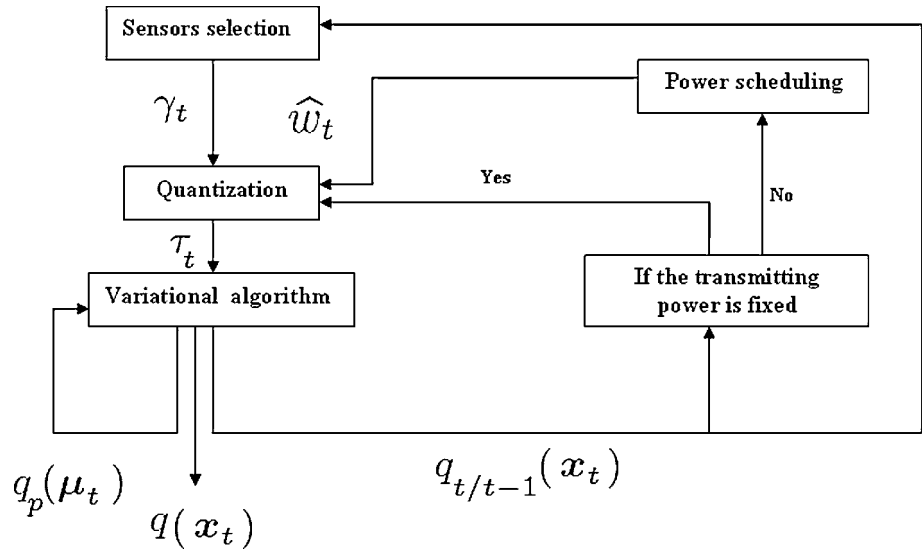
5.1 Analysis of tracking accuracy

To show the efficiency of the proposed method, we compare it with four previously proposed methods. The quantized proximity observation model, formulated in (2), was adopted for all the algorithms, except for the BVF algorithm, which is based on the binary proximity sensors.

One can notice from Fig. 7a that, even with abrupt changes in the target trajectory, the desired quality is achieved by the AQVF algorithm and outperforms the QVF-U algorithm. Figure 7b compares their tracking accuracies in terms of Root Mean Square Error (RMSE):

$$\text{RMSE} = \sqrt{E\left((x - \widehat{x})^2\right)}.$$

where x (resp. $\widehat{x}$) is the true trajectory (resp. the estimated trajectory).

The results confirm the impact of neglecting the transmission energy consumption in a WSN and the information relevance of sensor measurements. Unlike the QPF algorithm, the temporal dependence in the VF is reduced to one single Gaussian statistic instead of a huge number of particles. On the other hand, the precision of the PF algorithm depends on the choice of the importance sampling distribution. The VF yields an optimal choice of the sampling distribution over the target position x_t by minimizing the KL divergence. In fact, variational calculus leads to a simple Gaussian sampling distribution whose parameters (estimated iteratively) depends on the observed data. As can be expected, with the amount of particles increasing, the QPF algorithm demonstrates much more accurate tracking at the cost of a higher computation complexity. In particular, the computation time grows proportionally to the increment of the number of particles. The tracking

Fig. 7 **a** True and estimated trajectories with AQVF and QVF-U algorithms. **b** Mean square error comparison between AQVF and QVF-U algorithms
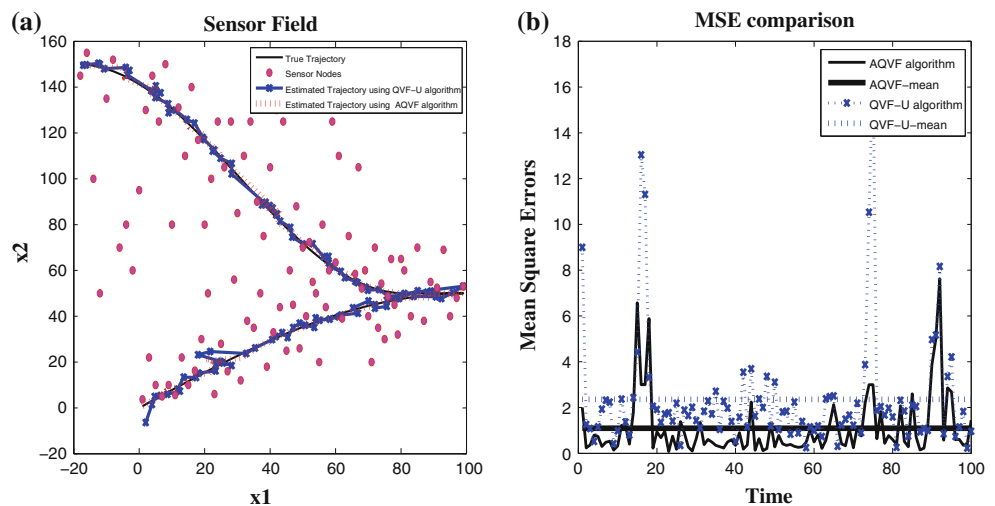
Fig. 8 **a** True and estimated trajectories with AQVF and BVF algorithms. **b** Mean square error comparison between AQVF and BVF algorithms
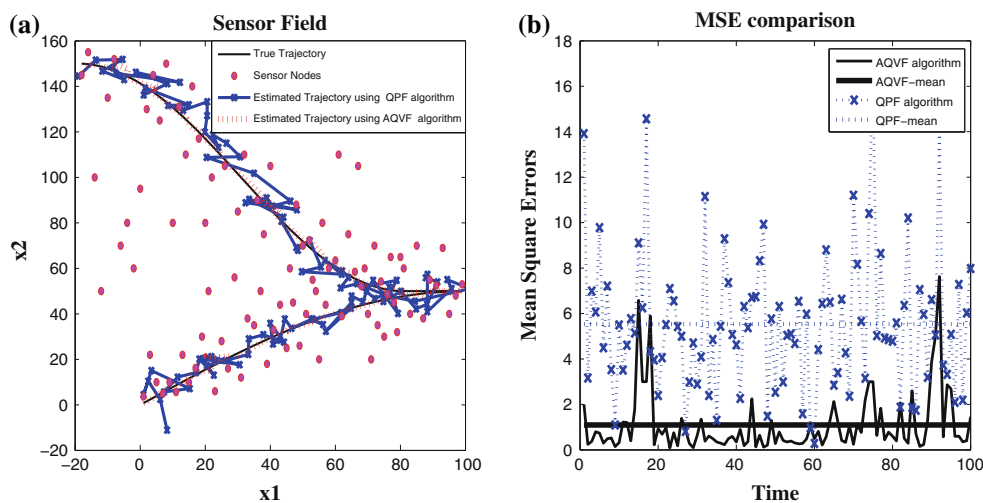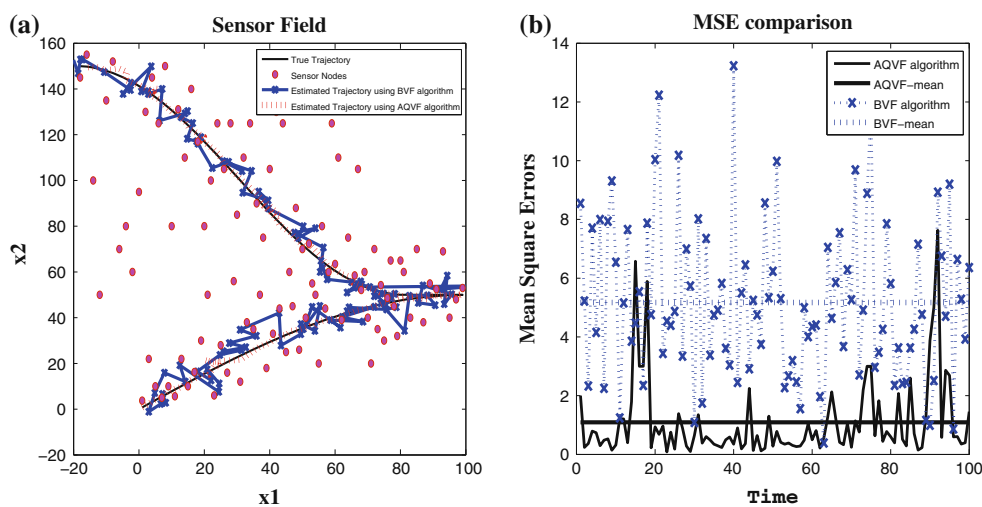

Fig. 9 **a** True and estimated trajectories with AQVF and QPF algorithms. **b** Mean square error comparison between AQVF and QPF algorithms

accuracies of the QPF and QGPF are compared to that of AQVF in Figs. 9, 10 respectively. The smaller RMSE of the AQVF in comparison with the two approximation methods confirms once again the effectiveness of the AQVF algorithm in terms of tracking accuracy.

5.2 Root mean square error (RMSE) analysis

The Root Mean Square Error (RMSE) of the above algorithms may depend on several factorssuch as the transmitting power between the candidate sensors and the *CH*, the nodes density, thesensing range, the pass losses as well as the sensor noise variances. The purpose of this subsectionis to study the impact of these factors when comparing the performance of the above mentionedtracking algorithms. Figure 11a shows the variation of the RMSE with respect to the nodes densityvarying in $\{50, \ldots, 200\}$. As can be expected, the RMSE decreases for all the algorithms

when the nodes density increases. One can also note that the proposed AQVF method outperforms all the other methods when varying the nodes density. It is also worth noting that its RMSE decreases more sharply than the other filtering methods. Figure 11b plots the RMSE versus the nodes noise variances varying in $\{0, \ldots, 0.25\}$ and Fig. 12a plots the RMSE with respect to the nodes transmitting power (varying in $\{50, \ldots, 200\}$). From the Fig. 12b, we can show that when sensing range varying in $\{5, \ldots, 13\}$, the error estimation decreases. These results confirm that the proposed method outperforms the classical methods when varying the simulation conditions.

5.3 Energy analysis

The energy consumption evaluation is done following the model proposed in [25]; in which we assume that: (1) the communication between the active sensors is via single

Fig. 10 a True and estimated trajectories with AQVF and QGPF algorithms. **b** Mean square error comparison between AQVF and QGPF algorithms
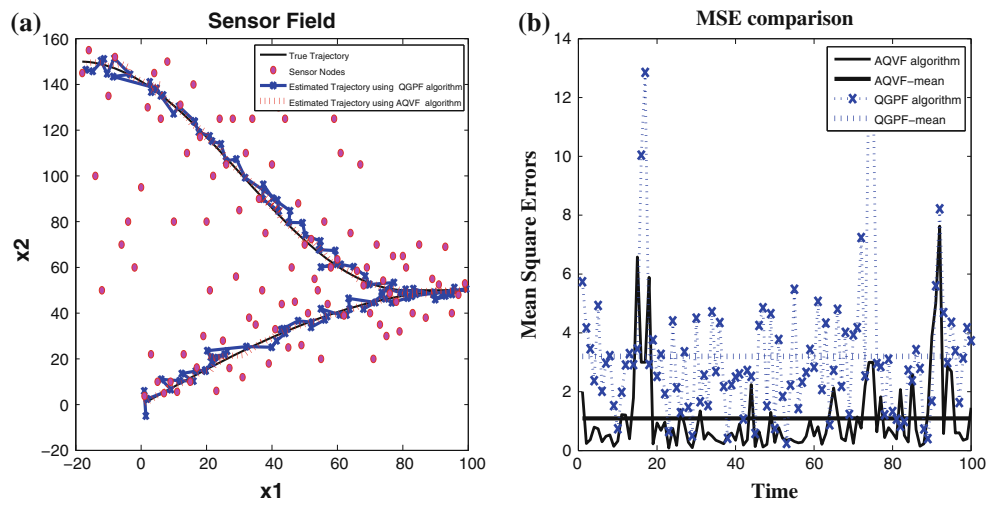

Fig. 11 a RMSE vesus nodes density. **b** RMSE versus nodes noise variances varying in $\{0, \ldots, 0.25\}$.
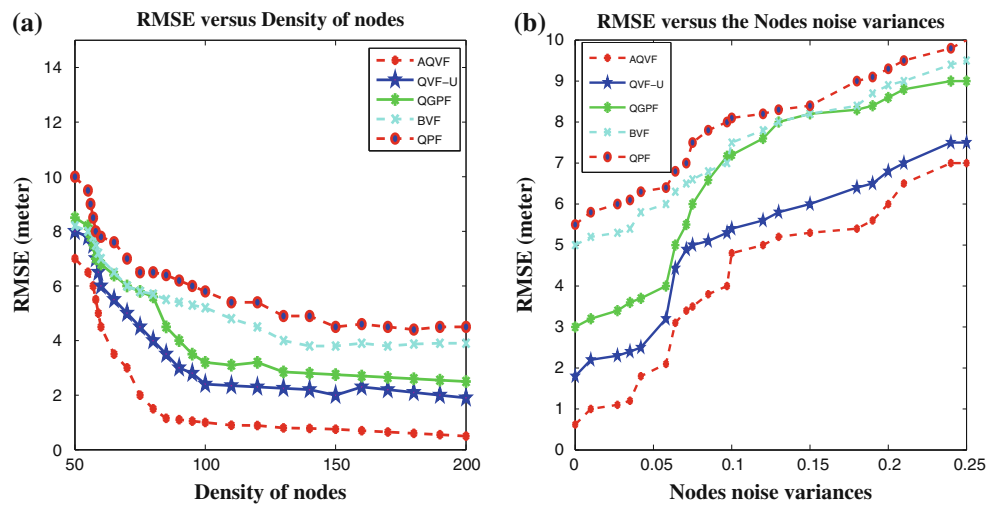

Fig. 12 a RMSE vesus transmitting power varying in $\{50, \ldots, 200\}$. **b** RMSE versus Sensing range varying in $\{5, \ldots, 13\}$.
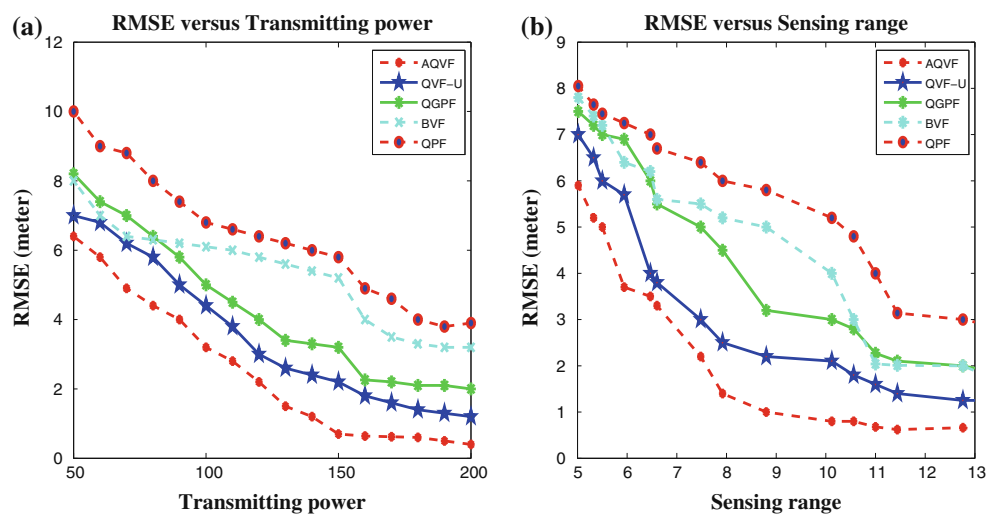
Table 1 Nodes communication comparison

Method	Nodes communication (bits)
AQVF	$L_{opt}N_a + 32 + 64$
QVF-U	$L_f N_a + 32 + 64$
BVF	$N_a + 32 + 64$
QPF	$L_f N_a + 32N_p + 16N_w$
QGPF	$L_f N_a + 32 + 64$

hop, (2) the energy consumed in scheduling and computing can be neglected relative to the energy consumed during communications.

The communication energy consists of three components: transmitter electronics energy, radio energy, and receiver electronics energy. The transmit power consumed at sensor (i), while transmitting data to CH is given by:

$$E_T = \epsilon_e + L^i \epsilon_a r_i^\lambda \tag{26}$$

where ϵ_a is the energy dissipated in Joules per bit per m^2, ϵ_e is energy consumed by the circuit per bit.

The receiving power consumed at ith sensor when receiving data from the CH, is given by:

$$E_R = L^i \epsilon_r \tag{27}$$

Similarly, the power consumed in sensing is defined by:

$$E_S = L^i \epsilon_s \tag{28}$$

where ϵ_s is the energy expending parameter for sensing L^i bits of data.

Considering the energy model, we choose $\epsilon_a = 100 \, \text{pJ/bit/m}^2$, $\epsilon_e = 50 \, \text{nJ/bit}$, $\epsilon_r = 135 \, \text{nJ/bit}$, $\epsilon_s = 50 \, \text{nJ/bit}$ [26]. Let N_p denote the number of particles, N_w the number of corresponding weights, L_{opt} the optimal bits number obtained by AQVF, and L_f the fixed bits number. The nodes communication of these algorithms were compared when a hand-off operation occurred. One can notice in Table 1 that the first components $L_f N_a$ are equal for the QVF-U, QPF and QGPF algorithms, since each activated sensor that detects the target transmits L_f bits of information to the CH. While for the AQVF algorithm, each

Fig. 13 Energy consumption comparison between AQVF and QVF-U algorithms for **a** $L = 3$. **b** $L = 4$
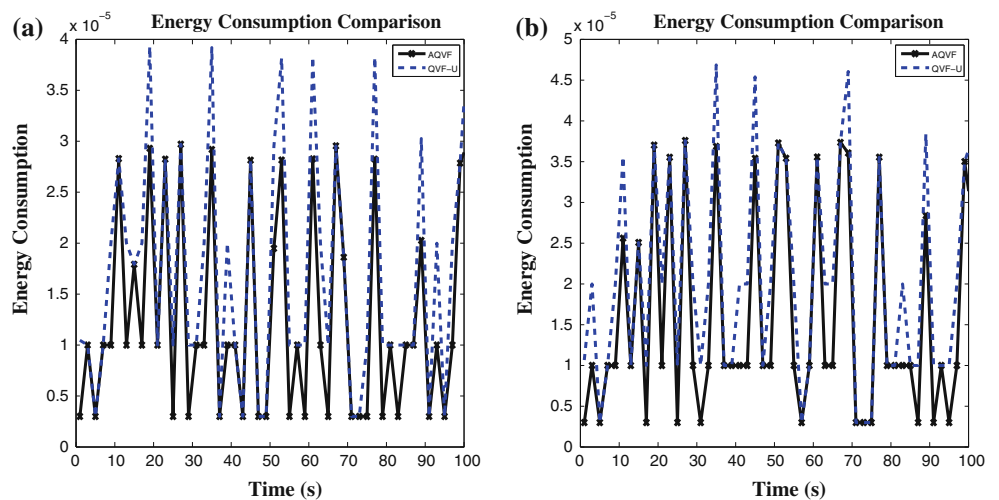

Fig. 14 Energy consumption comparison between AQVF and BVF algorithms for **a** $L = 3$. **b** $L = 4$
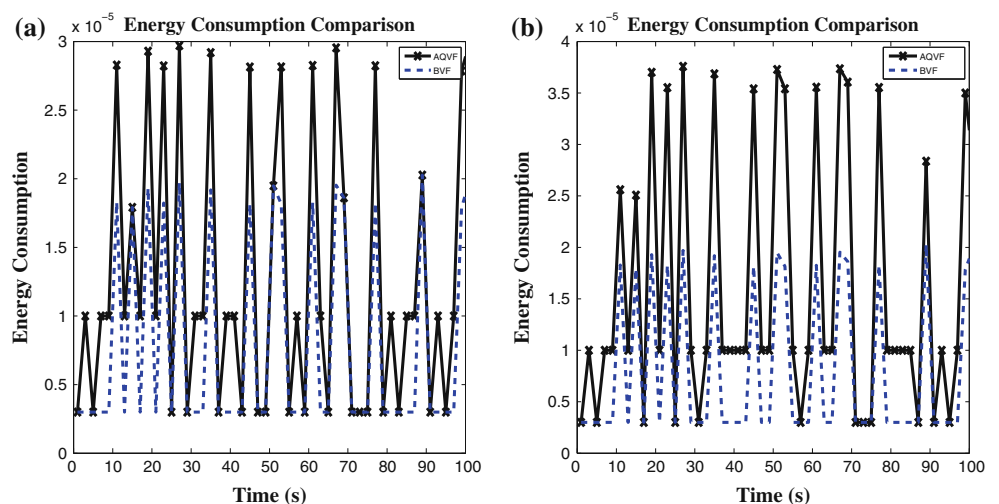
Fig. 15 Energy consumption comparison between AQVF and QPF algorithms for **a** $L = 3$. **b** $L = 4$
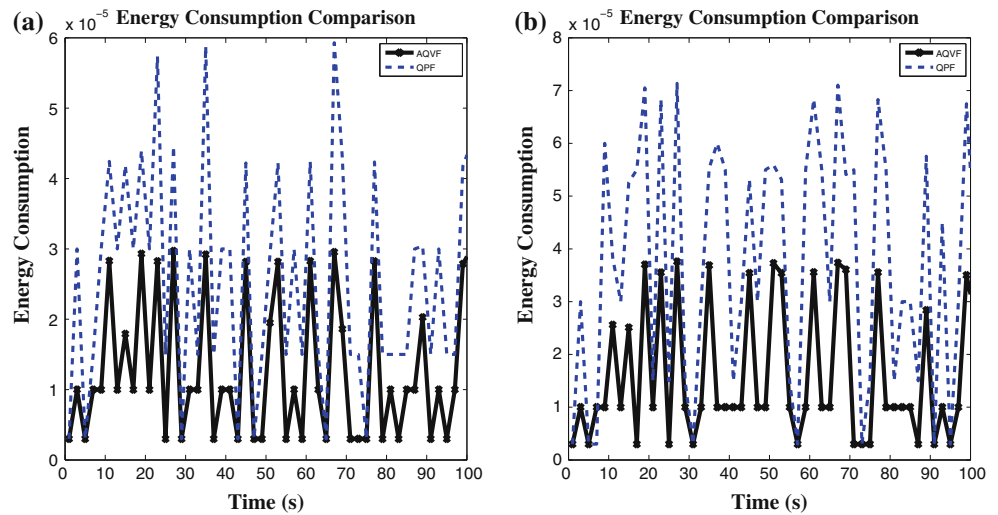
Fig. 16 Energy consumption comparison between AQVF and QGPF algorithms for **a** $L = 3$. **b** $L = 4$
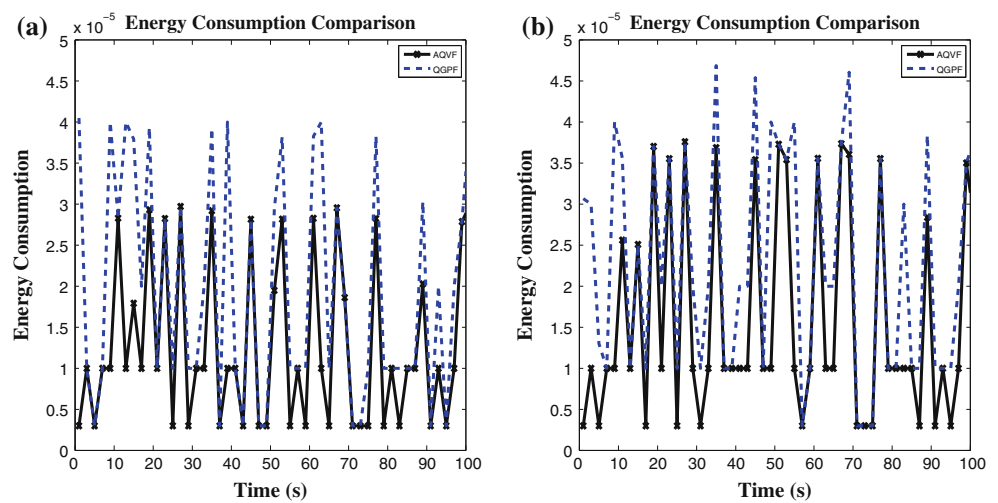
activated sensor can transmit L_{opt} (the optimal bits number) bits of data. However, for the BVF, each activated sensor transmits one bit of information to the *CH*. By approximating the filtering distribution with a single Gaussian statistic, the VF and GPF just have to transmit the expectation and the precision matrix. Nodes communication of the QPF mainly lies in communicating the particles and their corresponding weights, which is much greater than that of the VF and GPF. The nodes communication is shown in Table 1. From Figs. 13, 14, 15, and 16, wecan see that our protocol successfully balances the trade-off between the energy consumptionand the tracking accuracy even with several abrupt changes in the trajectory for all algorithms. These results confirm that the proposed method outperforms the classical algorithms

in terms of energy expenditure during the whole tracking process.

6 Conclusions

The main objective of this contribution is to show that data collection from sensors can beoptimized by adaptively controlling the quantization level. As for economical reasons, in the hardware layer, the deployment of quantized sensors greatly saves energy. In the software layer, the adaptive VF algorithm decreases the information exchanged between *CHs*. The proposedmethod provides not only the estimate of the target position using the variational filteringalgorithm but also gives the optimal number of

quantization bits per observation. This adaptive quantization is obtained by minimizing the Cramer–Rao bound if the transmitting power is fixed or by optimizing the power scheduling if the transmitting power is variable. The criteria computation is based on the target position predictive distribution provided by the variational filtering algorithm.

Appendix: Variational calculus

Assuming that the approximate distribution for the mean $\boldsymbol{\mu}_{t-1}$ follows a gaussian model $\left(q(\boldsymbol{\mu}_{t-1}) \sim \mathcal{N}\left(\boldsymbol{\mu}_{t-1}^{*}, \boldsymbol{\lambda}_{t-1}^{*}\right)\right)$ and taking into account the Gaussian transition of the mean $\left(p\left(\boldsymbol{\mu}_{t}|\boldsymbol{\mu}_{t-1}\right) \sim \mathcal{N}(\boldsymbol{\mu}_{t-1}, \bar{\lambda})\right)$, the predictive distribution of $\boldsymbol{\mu}_{t}$ is given by:

$$q_p(\boldsymbol{\mu}_t) = \int p(\boldsymbol{\mu}_t|\boldsymbol{\mu}_{t-1})q(\boldsymbol{\mu}_{t-1})d\boldsymbol{\mu}_{t-1}$$
$$\sim \mathcal{N}\left(\boldsymbol{\mu}_{t-1}^{*}, \left(\boldsymbol{\lambda}_{t-1}^{*}{}^{-1} + \bar{\lambda}^{-1}\right)^{-1}\right). \quad (29)$$

Let denote $\boldsymbol{\mu}_t^p$ and $\boldsymbol{\lambda}_t^p$ respectively the mean and the precision of the Gaussian distribution $q_p(\boldsymbol{\mu}_t)$: $q_p(\boldsymbol{\mu}_t) \sim \mathcal{N}\left(\boldsymbol{\mu}_t^p, \boldsymbol{\lambda}_t^p\right)$. According to the (6), the approximate distribution $q(\boldsymbol{\mu}_t)$ is expressed as:

$$q(\boldsymbol{\mu}_t) \propto \exp\langle \log p(z_{1:t}, \boldsymbol{\alpha}_t)\rangle_{q(\boldsymbol{x}_t)q(\boldsymbol{\lambda}_t)}$$
$$\propto \exp\langle \log p(\boldsymbol{\alpha}_t|z_t)\rangle_{q(\boldsymbol{x}_t)q(\boldsymbol{\lambda}_t)}$$
$$\propto \exp\langle \log p(z_t|\boldsymbol{x}_t) + \log p(\boldsymbol{x}_t|\boldsymbol{\mu}_t, \boldsymbol{\lambda}_t) + \log p(\boldsymbol{\lambda}_t)$$
$$+ \log q_p(\boldsymbol{\mu}_t)\rangle_{q(\boldsymbol{x}_t)q(\boldsymbol{\lambda}_t)}. \quad (30)$$

Therefore,

$$q(\boldsymbol{\mu}_t) \propto q_p(\boldsymbol{\mu}_t)\exp\langle \log p(\boldsymbol{x}_t|\boldsymbol{\mu}_t, \boldsymbol{\lambda}_t)\rangle_{q(\boldsymbol{x}_t)q(\boldsymbol{\lambda}_t)}$$
$$\propto q_p(\boldsymbol{\mu}_t)\exp\langle -\frac{1}{2}(\boldsymbol{x}_t - \boldsymbol{\mu}_t)^T \boldsymbol{\lambda}_t(\boldsymbol{x}_t - \boldsymbol{\mu}_t)\rangle_{q(\boldsymbol{x}_t)q(\boldsymbol{\lambda}_t)}$$
$$\propto q_p(\boldsymbol{\mu}_t)\exp -\frac{1}{2}\left\{ tr\left[\langle \boldsymbol{\lambda}_t\rangle_{q(\boldsymbol{\lambda}_t)}\langle (\boldsymbol{x}_t - \boldsymbol{\mu}_t)^T(\boldsymbol{x}_t - \boldsymbol{\mu}_t)\rangle_{q(\boldsymbol{x}_t)}\right]\right\}$$
$$\propto \exp -\frac{1}{2}\left[(\boldsymbol{\mu}_t - \boldsymbol{\mu}_t^p)^T \boldsymbol{\lambda}_t(\boldsymbol{\mu}_t - \boldsymbol{\mu}_t^p) - 2\boldsymbol{\mu}_t^T\langle \boldsymbol{\lambda}_t\rangle\langle \boldsymbol{x}_t\rangle\right.$$
$$\left. + \boldsymbol{\mu}_t^T\langle \boldsymbol{\lambda}_t\rangle\boldsymbol{\mu}_t\right], \quad (31)$$

yielding a Gaussian distribution $q(\boldsymbol{\mu}_t) = \mathcal{N}\left(\boldsymbol{\mu}_t^*, \boldsymbol{\lambda}_t^*\right)$. The first and the second derivatives of the logarithm of $q(\boldsymbol{\mu}_t)$ are expressed as:

$$\frac{\partial \log(q(\boldsymbol{\mu}_t))}{\partial \boldsymbol{\mu}_t} = -\frac{1}{2}\left[2\boldsymbol{\lambda}_t^p(\boldsymbol{\mu}_t - \boldsymbol{\mu}_t^p) - 2\langle \boldsymbol{\lambda}_t\rangle\langle \boldsymbol{x}_t\rangle + 2\langle \boldsymbol{\lambda}_t\rangle\boldsymbol{\mu}_t\right],$$

$$\frac{\partial^2 \log(q(\boldsymbol{\mu}_t))}{\partial \boldsymbol{\mu}_t \partial \boldsymbol{\mu}_t^T} = -\boldsymbol{\lambda}_t^p - \langle \boldsymbol{\lambda}_t\rangle,$$

the precision $\boldsymbol{\lambda}_t^*$ and the mean $\boldsymbol{\mu}_t^*$ of $q(\boldsymbol{\mu}_t)$ are obtained as follows:

$$\boldsymbol{\lambda}_t^* = \langle \boldsymbol{\lambda}_t\rangle + \boldsymbol{\lambda}_t^p, \quad \text{and} \quad \boldsymbol{\mu}_t^* = \boldsymbol{\lambda}_t^{*-1}\left(\langle \boldsymbol{\lambda}_t\rangle\langle \boldsymbol{x}_t\rangle + \boldsymbol{\lambda}_t^p\boldsymbol{\mu}_t^p\right). \quad (32)$$

The approximate separable distribution corresponding to $\boldsymbol{\lambda}_t$ can be computed following the same reasoning as above:

$$q(\boldsymbol{\lambda}_t) \propto \exp\langle \log p(\boldsymbol{\alpha}_t|z_t)\rangle_{q(\boldsymbol{x}_t)q(\boldsymbol{\mu}_t)}$$
$$\propto \exp\langle \log p(z_t|\boldsymbol{x}_t) + \log p(\boldsymbol{x}_t|\boldsymbol{\mu}_t, \boldsymbol{\lambda}_t) + \log p(\boldsymbol{\lambda}_t)$$
$$+ \log q_p(\boldsymbol{\mu}_t)\rangle_{q(\boldsymbol{x}_t)q(\boldsymbol{\mu}_t)}$$
$$\propto p(\boldsymbol{\lambda}_t)\exp\langle \log p(\boldsymbol{x}_t|\boldsymbol{\mu}_t, \boldsymbol{\lambda}_t)\rangle_{q(\boldsymbol{x}_t)q(\boldsymbol{\mu}_t)}$$
$$\propto \mathcal{W}_2(\bar{V}, \bar{n})|\boldsymbol{\lambda}_t|^{\frac{1}{2}}\exp$$
$$-\frac{1}{2}\left\{ tr\left[\boldsymbol{\lambda}_t\langle (\boldsymbol{x}_t - \boldsymbol{\mu}_t)^T(\boldsymbol{x}_t - \boldsymbol{\mu}_t)\rangle_{q(\boldsymbol{x}_t)q(\boldsymbol{\mu}_t)}\right]\right\}$$
$$\propto |\boldsymbol{\lambda}_t|^{\frac{\bar{n}+1-(2+1)}{2}}\exp$$
$$-\frac{1}{2}\left\{ tr\left[\boldsymbol{\lambda}_t\left(\langle \boldsymbol{x}_t\boldsymbol{x}_t^T\rangle - \langle \boldsymbol{x}_t\rangle\langle \boldsymbol{\mu}_t\rangle^T\right.\right.\right.$$
$$\left.\left.\left. - \langle \boldsymbol{\mu}_t\rangle\langle \boldsymbol{x}_t\rangle^T + \langle \boldsymbol{\mu}_t\boldsymbol{\mu}_t^T\rangle + \bar{V}^{-1}\right)\right]\right\}, \quad (33)$$

which yields a Wishart distribution $\mathcal{W}_2(V^*, n^*)$ for the precision matrix $\boldsymbol{\lambda}_t$ with the following parameters:

$$\begin{cases} n^* = \bar{n} + 1, \\ V^* = \left(\langle \boldsymbol{x}_t\boldsymbol{x}_t^T\rangle - \langle \boldsymbol{x}_t\rangle\langle \boldsymbol{\mu}_t\rangle^T - \langle \boldsymbol{\mu}_t\rangle\langle \boldsymbol{x}_t\rangle^T + \langle \boldsymbol{\mu}_t\boldsymbol{\mu}_t^T\rangle + \bar{V}^{-1}\right)^{-1}. \end{cases} \quad (34)$$

Finally, the approximate distribution $q(\boldsymbol{x}_t)$ has the following expression:

$$q(\boldsymbol{x}_t) \propto \exp\langle \log p(\boldsymbol{\alpha}_t|z_t)\rangle_{q(\boldsymbol{\mu}_t)q(\boldsymbol{\lambda}_t)}$$
$$\propto \exp\langle \log p(z_t|\boldsymbol{x}_t) + \log p(\boldsymbol{x}_t|\boldsymbol{\mu}_t, \boldsymbol{\lambda}_t) + \log p(\boldsymbol{\lambda}_t)$$
$$+ \log q_p(\boldsymbol{\mu}_t)\rangle_{q(\boldsymbol{\mu}_t)q(\boldsymbol{\lambda}_t)}$$
$$\propto p(z_t|\boldsymbol{x}_t)\exp\langle \log p(\boldsymbol{x}_t|\boldsymbol{\mu}_t, \boldsymbol{\lambda}_t)\rangle_{q(\boldsymbol{\mu}_t)q(\boldsymbol{\lambda}_t)}$$
$$\propto p(z_t|\boldsymbol{x}_t)$$
$$\exp -\frac{1}{2}\left\{ tr\left[\langle \boldsymbol{\lambda}_t\rangle_{q(\boldsymbol{\lambda}_t)}\langle (\boldsymbol{x}_t - \boldsymbol{\mu}_t)^T(\boldsymbol{x}_t - \boldsymbol{\mu}_t)\rangle_{q(\boldsymbol{\mu}_t)}\right]\right\}$$
$$\propto p(z_t|\boldsymbol{x}_t)\mathcal{N}(\langle \boldsymbol{\mu}_t\rangle, \langle \boldsymbol{\lambda}_t\rangle), \quad (35)$$

which does not have a closed form. Therefore, contrary to the cases of the mean $\boldsymbol{\mu}_t$ and the precision $\boldsymbol{\lambda}_t$, in order to compute the expectations relative to the distribution $q(\boldsymbol{x}_t)$, one has to resort to the importance sampling method where samples are generated according to the Gaussian $\mathcal{N}(\langle \boldsymbol{\mu}_t\rangle, \langle \boldsymbol{\lambda}_t\rangle)$ and then weighted according to the likelihood $p(z_t|\boldsymbol{x}_t)$.

References

1. Chen, Y., & Zhao, Q. (2005). On the lifetime of wireless sensor networks. *IEEE Communications Letters, 9*(11), 976–978.

2. Gray, R. M. (2006). Quantization in task-driven sensing and distributed processing. In *IEEE International conference on acoustics, speech, and signal processing* (Vol. 5, pp. 1049–1052).

3. Luo, X., & Giannakis, G. (2008). Energy-constrained optimal quantization for wireless sensor networks. *EURASIP Journal on Advances in Signal Processing*, 1–12.

4. Mansouri, M., Ouchani, I., Snoussi, H., & Richard, C. (2009). Cramer–Rao bound-based adaptive quantization for target tracking in wireless sensor networks. In *IEEE/SP workshop on statistical signal processing, 2009. SSP'09*.

5. Ribeiro, A., Giannakis, G. B., & Roumeliotis, S. I. (2006). SOI-KF: Distributed Kalman filtering with low-cost communications using the sign of innovation. *IEEE Transactions on Signal Processing, 54*(12), 4782–4795.

6. Fang, J., & Li, H. (2008). Distributed adaptive quantization for wireless sensor networks: From delta modulation to maximum likelihood. *Signal Processing, IEEE Transactions on, 56*(10), 5246–5257.

7. Pattem, S., Poduri, S., & Krishnamachari, B. (2003). Energy-quality tradeoffs for target tracking in wireless sensor networks. In *Information processing in sensor networks* (pp. 553–553). Springer: Berlin.

8. Brooks, R., Ramanathan, P., & Sayeed, A. (2003). Distributed target classification and tracking in sensor networks. *Proceedings of the IEEE, 91*(8), 1163–1171.

9. Yang, H., & Sikdar, B. (2003). A protocol for tracking mobile targets using sensor networks. In *Sensor network protocols and applications, 2003. Proceedings of the First IEEE. 2003 IEEE international workshop on IEEE* (pp. 71–81).

10. Julier, S., & Uhlmann, J. (2004). Unscented filtering and non-linear estimation. In *Proceedings of the IEEE* (Vol. 92, pp. 401–422).

11. Djuric, P., Kotecha, J. Z. J., Huang, Y., Ghirmai, T., Bugallo, M., & Miguez, J. (2003). Particle filtering. *IEEE Signal Processing Magazine, 20*, 19–38.

12. Snoussi, H., & Richard, C. (2006). Ensemble learning online filtering in wireless sensor networks. In *IEEE ICCS International conference on communications systems*.

13. Kotecha, J., & Djuric, P. (2003). Gaussian particle filtering. *IEEE Transactions on Signal Processing, 51*(10), 2592–2601.

14. Kotecha, J., & Djuric, P. (2003). Gaussian sum particle filtering. *IEEE Transactions on Signal Processing, 51*(10), 2602–2612.

15. Ihler, A., Fisher, J., III., Willsky, A. (2005). Particle filtering under communications constraints. In *Proceedings statistical signal processing (SSP) 2005*.

16. Teng, J., Snoussi, H., & Richard, C. (2007). Binary variational filtering for target tracking in wireless sensor networks. In *IEEE workshop on statistical signal processing* (pp. 685–689).

17. Djurić, P., Vemula, M., & Bugallo, M. (2005). Tracking with particle filtering in tertiary wireless sensor networks. In *ICASSP* (pp. 18–23). Philadelphia.

18. Yick, J., Mukherjee, B., & Ghosal, D. (2005). Analysis of a prediction-based mobility adaptive tracking algorithm. In *Proceedings of the IEEE second international conference on broadband networks (BROADNETS)*. Boston.

19. Chhetri, A., Morrell, D., & Papandreou-Suppappola, A. (2005). Energy efficient target tracking in a sensor network using non-myopic sensor scheduling. In *Information fusion, 2005 8th international conference on* (Vol. 1).

20. Vermaak, J., Lawrence, N., & Perez, P. (2003). Variational inference for visual tracking. In *Proceedings of 2003 IEEE computer society conference on computer vision and pattern recognition, 2003* (Vol. 1).

21. Snoussi, H., & Richard, C. (2006). Ensemble learning online filtering in wireless sensor networks. In *10th IEEE Singapore international conference on communication systems, 2006. ICCS 2006* (pp. 1–5).

22. Chen, W., Hou, J., & Sha, L. (2004). Dynamic clustering for acoustic target tracking in wireless sensor networks. *IEEE transactions on mobile computing* (pp. 258–271).

23. Cui, S., Goldsmith, A., & Bahai, A. (2005). Energy-constrained modulation optimization. *IEEE Transactions on Wireless Communications, 4*(5), 2349–2360.

24. Teng, J., Snoussi, H., & Richard, C. (2007). Binary variational filtering for target tracking in sensor networks. In *IEEE/SP 14th workshop on statistical signal processing, 2007. SSP'07* (pp. 685–689).

25. Heinzelman, W., Chandrakasan, A., & Balakrishnan, H. (2000). Energy-efficient communication protocol for wireless microsensor networks. In *Proceedings of the 33rd Hawaii international conference on system sciences* (Vol. 8, pp. 8020). Citeseer.

26. Teng, J., Snoussi, H., & Richard, C. (2007). Prediction-based proactive cluster target tracking protocol for binary sensor networks. In *2007 IEEE international symposium on signal processing and information technology* (pp. 234–239).

Author Biographies

Majdi Mansouri was born November 11, 1982 in Kasserine, Tunisia. He received the Engineer Diploma in "Telecommunications" from High School of Communications of Tunis (SUP'COM) in 2006 and the Master Diploma in "Signal and Image processing" from High school of Electronic, Informatique and Radiocommunications in Bordeaux (ENSEIRB) in 2008. He is PhD student at Troyes University of Technology, France, since October 2008. His current research interests include statistical signal processing and Wireless Sensors Networks. He is the author of over 20 papers.

Ouachani Ilham was born in Paris, France, in 1976. She received the diploma degree in electrical engineering from The Ecole supérieure de Communication de Tunis (Sup'Com), Tunisie in 2000. Then, she received the DEA degree from ParisTech Paris , and the Ph.D. in signal processing from the University of Paris-sud, Orsay, France in 2001 and 2005, respectively. Between 2005 and 2006, she was a teaching assistant in with the University of Paris-sud and the Conservatoire National des Arts et Métiers de Paris. Since september 2006, she is associate professor at the Institut Supérieur d'Informatique et des Techniques de Communication, in Hammam. Sousse, Tunisia. She has won the AUF grant and she has spent 6 months as visiting scientist at the LM2S laboratory in the University of Technology of Troyes, France, in 2009. Her research interests include MIMO systems, capacity calculation, OFDM, relay channels, digital communication in wireless sensor networks, She is

author of several research papers in journals and international conferences.

Hichem Snoussi was born in Bizerta, Tunisia, in 1976. He received the diploma degree in electrical engineering from the Ecole Superieure d'Electricite (Supelec), Gif-sur-Yvette, France, in 2000. He also received the DEA degree and the Ph.D. in signal processing from the University of Paris-Sud, Orsay, France, in 2000 and 2003 respectively. He has obtained the HdR from the University of Technology of Compiègne in 2009. Between 2003 and 2004, he was postdoctoral researcher at IRCCyN, Institut de Recherches en Communications et Cybernétiques de Nantes. He has spent short periods as visiting scientist at the Brain Science Institute, RIKEN, Japan and Olin Neuropsychiatry Research Center at the Institute of Living in USA. Between 2005 and 2010, he has been associate professor at the University of Technology of Troyes. Since September 2010, he has been appointed a Full Professor position at the same university. He is in charge of the regional research program S3 (System Security and Safety) of the CPER 2007-2013 and the CapSec plateform (wireless embedded sensors for security). He is the principal investigator of an ANR-Blanc project (mv-EMD), a CRCA project (new partnership and new technologies) and a GDR-ISIS young researcher project. He is partner of many ANR projects, GIS, strategic UTT programs. He obtained the national doctoral and research supervising award PEDR 2008-2012.

Cédric Richard was born January 24, 1970 in Sarrebourg, France. I received the Dipl.-Ing. and the M.S. degrees in 1994 and the Ph.D. degree in 1998 from the University of Technology of Compiegne, France, all in Electrical and Computer Engineering. From 1999 to 2003, he was an Associate Professor at the University of Technology of Troyes, France. From 2003 to 2009, he was a Full Professor at the Institut Charles Delaunay (CNRS FRE 2848) at the UTT, and the supervisor of a group consisting of 60 researchers and Ph.D. In winter 2009 and autumn 2010, he was a Visiting Researcher with the Department of Electrical Engineering, Federal University of Santa Catarina (UFSC), Florianopolis, Brazil. Cédric Richard is a junior member of the Institut Universitaire de France since october 2010. Since September 2009, Cédric Richard is a Full Professor at Fizeau Laboratory (CNRS UMR 6525, Observatoire de la Cote d'Azur), University of Nice Sophia-Antipolis, France. His current research interests include statistical signal processing and machine learning. Prof. Cédric Richard is the author of over 100 papers. He was the General Chair of the XXIth francophone conference GRETSI on Signal and Image Processing that was held in Troyes, France, in 2007, and of the IEEE International Workshop on Statistical Signal Processing that will be held in Nice in 2011. Since 2005, he is a member of the board of the federative CNRS research group ISIS on Information, Signal, Images and Vision. He is a member of GRETSI association board and of the EURASIP society, and Senior Member of the IEEE. Cédric Richard serves as an Associate Editor of the IEEE Transactions on Signal Processing since 2006, and of the EURASIP Signal Processing Magazine since 2009. In 2009, he was nominated liaison local officer for EURASIP, and member of the Signal Processing Theory and Methods (SPTM) Technical Committee of the IEEE Signal Processing Society.